Plasma Physics Reports, Vol. 24, No. 12, 1998, pp. 1000–1007. Translated from Fizika Plazmy, Vol. 24, No. 12, 1998, pp. 1070–1077.
Original Russian Text Copyright © 1998 by Akhmetov, Davydenko, Kabantsev, Reva, Sokolov, Taskaev.

MAGNETIC CONFINEMENT SYSTEMS

Magnetic-Field Fluctuations in the Startup Plasma of the AMBAL-M Device

T. D. Akhmetov, V. I. Davydenko, A. A. Kabantsev, V. B. Reva, V. G. Sokolov, and S. Yu. Taskaev

Budker Institute of Nuclear Physics, Siberian Division, Russian Academy of Sciences, pr. akademika Lavrent'eva 11, Novosibirsk, 630090 Russia

Received September 22, 1997

Abstract— Fluctuations of the azimuthal and radial magnetic field in the startup plasma of the end system of the AMBAL-M tandem mirror system are measured by magnetic probes. An analysis of the spectra and radial profiles of the magnetic-field and density fluctuations shows that there is a correlation between these quantities, which can be explained in terms of the Kelvin–Helmholtz instability in a plasma stream flowing out of the gas-discharge source. The characteristic parameters of the stream inhomogeneities are estimated. The radial profile of the particle flux is determined from simultaneous measurements of the plasma density and radial magnetic field. The diffusion coefficient related to magnetic-field fluctuations is estimated.

1. INTRODUCTION

In experiments carried out in the first stage of the AMBAL-M tandem mirror system, a substantial (to 1.6 kA) longitudinal electron current flowing in the startup plasma and the plasma transport across the magnetic field with a diffusion coefficient larger than the classical ambipolar diffusion coefficient by two orders of magnitude were observed. In order to study the properties of the longitudinal current and the magnetic-field fluctuations and to determine the contribution from the latter to the plasma transport, we performed measurements with the help of movable magnetic probes.

The device was described in detail in [1, 2]. By using a gas-discharge plasma source, a hot target plasma is produced in an axisymmetric end mirror device (end cell) with magnetic field of 7.5 kG in the central plane. The plasma radius is 10 cm, the density is up to 6×10^{12} cm^{-3}, the ion temperature is $T_i \approx 200$ eV, and electron temperature is $T_e \approx 50$ eV. The main experimental results are presented in [3].

The longitudinal electron current flowing along the plasma stream during the discharge in the plasma source was studied experimentally in [4]. Here, we study magnetic-field fluctuations and related plasma transport in the startup plasma of the AMBAL-M device by using movable magnetic probes.

Interest in magnetic-field fluctuations is motivated by theoretical studies in which it has been shown that these fluctuations can substantially enhance heat and particle transport across the magnetic field due to the particle drift along the magnetic surfaces perturbed by fluctuations. A large number of papers devoted to direct measurements of the magnetic-field fluctuations and to studies of their spectral and mode composition have been published (see, e.g., [5–7]). One of the first experiments on the contact measurements of magnetic-field fluctuations in a tokamak plasma by small, multiturn coils placed inside an insulating shell was described in [5]. At present, direct measurements of heat and particle fluxes by determining the correlation between such plasma parameters as the density, electric and magnetic fields, and so on are being carried out (see [8–10]).

In this paper, simultaneous measurements of both the plasma density by a Langmuir probe and the radial magnetic field by a magnetic probe are carried out; based on these measurements, the radial profile of the particle flux is derived. The diffusion coefficient related to magnetic-field fluctuations is estimated to be $D_\perp \leqslant 0.3 \times 10^4$ cm^2/s, which is at least an order of magnitude less than the total diffusion coefficient observed in the experiment. Therefore, a conclusion is made on the dominant role of electrostatic fluctuations in the plasma transport across the magnetic field.

An analysis of the spectra and radial profiles of magnetic-field and density fluctuations shows that there is a correlation between these quantities in the plasma stream, which can be explained in terms of the Kelvin–Helmholtz instability (KHI). The characteristic parameters of plasma inhomogeneities are estimated.

2. SCHEMATIC OF MAGNETIC-PROBE MEASUREMENTS

The schematic of an axisymmetric end mirror device, which is the first stage (end cell) of the AMBAL-M device, is presented in Fig. 1, in which the magnetic field lines emerging from the plasma source are also shown. A plasma with a characteristic temper-

1063-780X/98/2412-1000$15.00 © 1998 МАИК Наука/Interperiodica Publishing

ature of ~10 eV and density $n \approx 2 \times 10^{14}$ cm^{-3} flows out of the source with a flow velocity on the order of thermal velocity and propagates along the magnetic field lines.

The magnetic field components are measured by magnetic probes, which are small, multiturn coils placed inside an insulating shell made from boron nitride. The probes are mounted on movable insulated rods, which are inserted into the plasma with the help of a coordinate unit.

3. PARTICLE FLUX ACROSS THE MAGNETIC FIELD

It is known that plasma instabilities can substantially enhance heat and particle transport across the magnetic field. The onset of instability results in the motion of particles across the magnetic field; the displacement of a particle along the plasma density gradient can be much higher than the Larmor radius. Collective oscillations of plasma particles result in the plasma transport along the macroscopic gradient. This effect has been observed in experiments carried out in the end system of the AMBAL-M device, in which the plasma is produced by an annular gas-discharge source. Due to the onset of the electrostatic KHI, the coefficient of the plasma diffusion across the magnetic field reaches $D_\perp \sim 10^5$ cm^2/s [11]. Nevertheless, the role of the observed magnetic-field fluctuations in the transport processes in the AMBAL-M device remains unclear. Therefore, we have performed the local measurements of the particle flux by magnetic and Langmuir probes.

Let us consider the radial particle flux $\Gamma_r = nv_r$, where n and v_r are the plasma density and radial velocity, respectively. In a turbulent plasma, each quantity can be written as a sum of time-averaged and fluctuating parts, $n = \langle n \rangle + \tilde{n}$, where $\langle \ldots \rangle$ means averaging over a time interval larger than the characteristic fluctuation period, so $\langle \tilde{n} \rangle = 0$, and $\langle n \rangle$ is the average density. The total time-averaged particle flux can be written as $\Gamma_r = \langle (\langle n \rangle + \tilde{n})(\langle v_r \rangle + \tilde{v}_r) \rangle = \langle n \rangle \langle v_r \rangle + \langle \tilde{n}\, \tilde{v}_r \rangle$. Therefore, the turbulent flux depends on the correlation between the density and radial-velocity fluctuations, $\Gamma_r^{\text{turb}} = \langle \tilde{n}\, \tilde{v}_r \rangle$.

The particle velocity includes the velocity of the free motion along the magnetic field and the velocity of the drift in the crossed fields

$$\mathbf{v} = \mathbf{u}_{0\|} + c\frac{\mathbf{E} \times \mathbf{B}}{B^2},$$

where $u_{0\|}$ is the velocity of the guiding center of a particle along the magnetic field direction. Note that we neglect both the drift related to the curvature of the magnetic field lines and the gradient drift, because these are relatively small; we also assume that the paraxial approximation is valid and the magnetic field

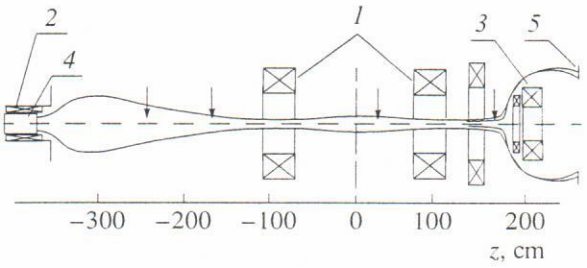

Fig. 1. Schematic of the end system of the AMBAL-M device and the magnetic field line emerging from the plasma source: (*1*) coils of the end cell, (*2*) solenoid of the plasma source, (*3*) semicusp coil, (*4*) plasma source, and (5) plasma collector. Arrows mark the cross sections in which the magnetic probe measurements are performed.

of the longitudinal current is low compared to the vacuum magnetic field: $B_{0r}, B_{0\varphi} \ll B_{0z}$. From here on, we use cylindrical coordinates with the z-axis directed along the device axis. Under the conditions of our experiment, all components of the electric field except the azimuthal component can be neglected. Then, for the fluctuating component of the radial velocity we have

$$\tilde{v}_r \approx u_{0\|}\frac{\tilde{B}_r}{B} + c\frac{\tilde{E}_\varphi}{B},$$

and for the turbulent particle flux we have

$$\Gamma_r^{\text{turb}} = \langle \tilde{n}\tilde{v}_r \rangle = u_{0\|}\frac{\langle \tilde{n}\tilde{B}_r \rangle}{B} + \frac{c\langle \tilde{n}\tilde{E}_\varphi \rangle}{B}. \qquad (1)$$

Electrostatic transport is associated with the second term on the right-hand side of (1), whereas the first term corresponds to the magnetic transport. In the case of ambipolar diffusion, the transport is characterized by the ion velocity $u_{0\|}$ in (1). It is seen from (1) that the transport depends not only on the fluctuation amplitude, but also on the correlation between different fluctuating quantities.

To clearly understand the mechanism for magnetic transport, let us consider the free particle motion along the magnetic field, on which transverse perturbations are superimposed. Because of these perturbations, a particle acquires the velocity component $\tilde{v}_r(\tilde{B}) = v_\| \tilde{B}_r/B$; as a result, the fast particle motion along the magnetic field is partially transformed into radial motion. Due to the overlapping of adjacent magnetic surfaces, the particle can go to another field line, which results in transport across the magnetic field.

If the correlation between fluctuating quantities is complete, then from (1) we can obtain the upper estimates for the particle fluxes. Denoting the particle fluxes related to fluctuations of electrostatic and mag-

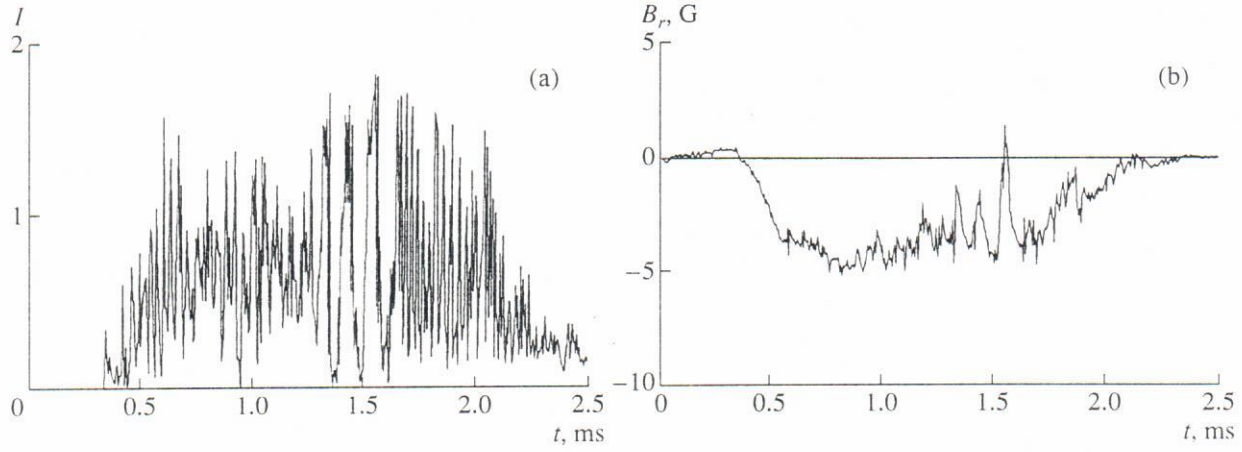

Fig. 2. Typical time dependences of (a) the probe current and (b) the radial magnetic field at $z = -243$ cm and $r = 16$ cm (n [cm^{-3}] ≈ $I \times 10^{13}$).

netic fields as Γ_E and Γ_B, respectively, we obtain $\Gamma_E \sim c\tilde{n}\tilde{E}_\varphi/B$ and $\Gamma_B \sim u_{0\|}\tilde{n}\tilde{B}_r/B$. The ratio of these fluxes is

$$\frac{\Gamma_B}{\Gamma_E} \sim \frac{u_{0\|}\tilde{B}_r}{c\tilde{E}_\varphi}. \quad (2)$$

The electrostatic-field fluctuations can be estimated as $\tilde{E}_\varphi \sim m\tilde{\phi}/a$, where m is the azimuthal mode number, a is the plasma radius, and $\tilde{\phi}$ is the amplitude of the fluctuation potential. Substituting in (2) the experimentally measured values of the plasma parameters in the cross section $z = -243$ cm of the transport region (the region extended from the plasma source to the input mirror of the end cell): $m \sim 1$–5, $a \sim 20$ cm, $\tilde{\phi} \sim 50$ V, $\tilde{B}_r \sim 2$ kG, $B \sim 1$ kG, $u_{0\|} \sim 3 \times 10^6$ cm/s, we obtain $\Gamma_B/\Gamma_E \sim 0.04/m \ll 1$; i.e., in this cross section, the particle flux related to magnetic-field fluctuations is much less than that related to electrostatic fluctuations. From the expression for Γ_E we can also obtain the upper estimate of the diffusion coefficient $D_\perp \sim |\Gamma_E/(dn/dr)| \sim c\tilde{E}_\varphi \Delta r/B \sim cm\tilde{\phi}\Delta r/(aB) \sim 2 \times 10^5$ cm^2/s. This value is overestimated, because we assume the correlation between $\tilde{n}$ and $\tilde{E}_\varphi$ to be total.

Electrostatic transport was studied in detail in [12], and, in this paper, we consider magnetic transport. It follows from the above considerations that, in order to experimentally determine the turbulent particle flux, it is necessary to simultaneously measure the density fluctuations and radial magnetic field at the same point and to average their product over time. In our experiment, the plasma density was measured by a Langmuir probe operating in the ion-current saturation regime, and the radial magnetic field was measured by a magnetic probe that was located close to the Langmuir probe. Figure 2 shows the time dependences of the Langmuir-probe current and the radial magnetic field. The bias voltage $U_b = -70$ V was applied to the probe to prevent electrons from arriving at the probe. It is seen that the probe current suffers substantial (up to 100%) fluctuations with respect to its average value. Assuming that the probe ion current is proportional to the plasma density, we will take the properly normalized current as the plasma density.

The oscillograms of the plasma density and the radial magnetic field are presented in Fig. 3 for the time interval from 900 to 1900 μs. It is seen on such an extended scale that, beginning from approximately 1000 μs, the low-frequency ($\nu \sim 10$ kHz) oscillations of the plasma density and the magnetic field appear simultaneously. Both the amplitude of these oscillations and the intervals between neighboring maximums increase with time. This pattern breaks at $t \approx 1700$ μs, when the plasma source is switched off.

An analysis of the fluctuation spectra of the plasma density and magnetic field shows that the highest power falls within the frequency range $\nu \leqslant 100$ kHz; the individual maximums corresponding to KHI are seen in the spectra presented in Fig. 4. It is also seen that the peaks in the spectra of plasma density and magnetic field occur at the same frequencies; this is evidence for the correlation between the measured quantities.

The value of $\langle \tilde{n}(t)\tilde{B}_r(t)\rangle$ can be found by direct averaging over the given time interval; however, it is more convenient to go over to the Fourier transforms. If $\tilde{n}(\omega) \equiv |\tilde{n}(\omega)|\exp(i\theta_n(\omega))$ and $\tilde{B}_r(\omega) \equiv |\tilde{B}_r(\omega)|\exp(i\theta_B(\omega))$ are the Fourier transforms of the

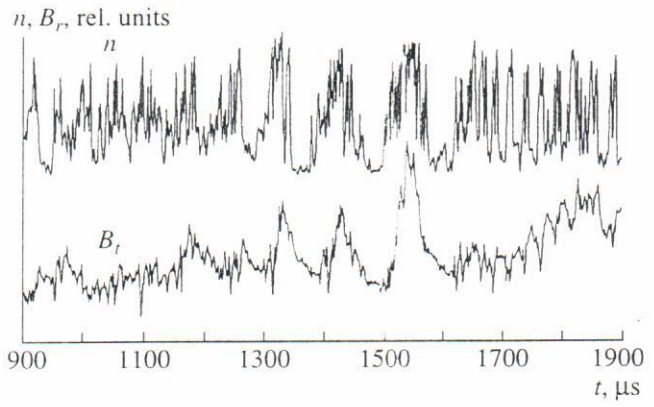

Fig. 3. Dependences $I_{probe}(t)$ and $B_r(t)$ from Fig. 2 (z = –243 cm and r = 16 cm) on an extended time scale.

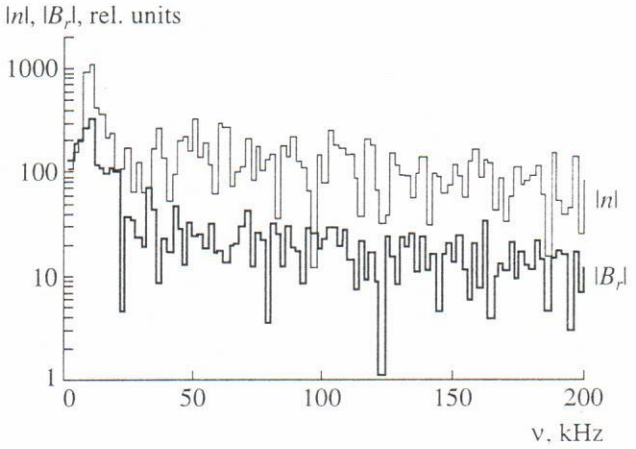

Fig. 4. Spectra of fluctuations of the density and radial magnetic field at z = –243 cm and r = 16 cm.

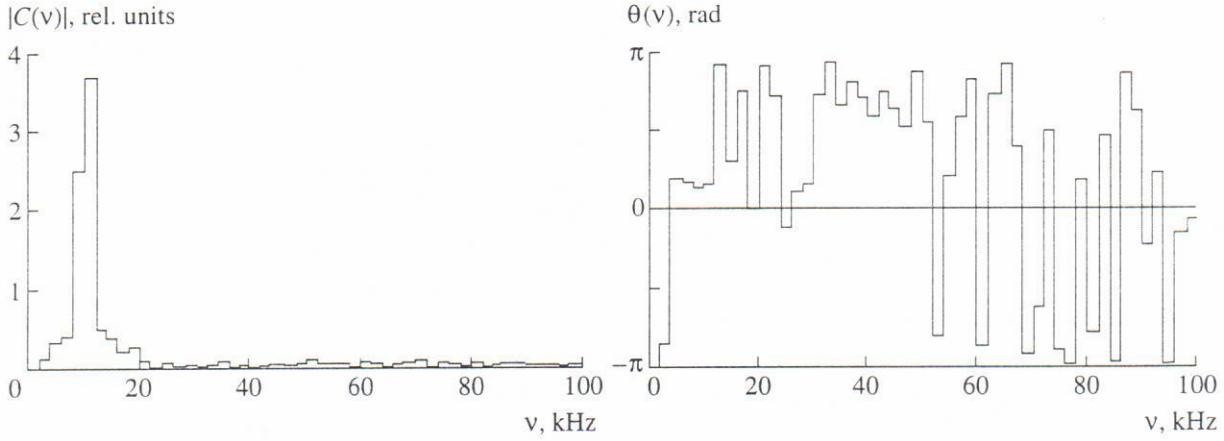

Fig. 5. The cross spectrum $C(\omega)$ of density and radial magnetic field fluctuations and the phase difference between them at z = –243 cm and r = 16 cm.

initial signals, then we have

$$\langle \tilde{n}(t)\tilde{B}_r(t)\rangle = \int_{-\infty}^{\infty} \tilde{n}^*(\omega)\tilde{B}_r(\omega)d\omega = 2\int_0^{\infty} |C(\omega)|\cos\theta(\omega)d\omega, \quad (3)$$

where $C(\omega) = \tilde{n}^*(\omega)\tilde{B}_r(\omega)$, $\theta(\omega) = \theta_B(\omega) - \theta_n(\omega)$ is the phase shift between oscillations of the magnetic field and plasma density. Such a representation allows us to determine what frequencies contribute most to the particle transport. For the particle flux, we obtain $\Gamma_B^{turb} = \int_0^{\infty} \Gamma(\omega)d\omega$, where $\Gamma(\omega) = 2u_{0\|}|C(\omega)|\cos\theta(\omega)/B$. Figure 5 presents the functions $|C(\omega)|$ and $\theta(\omega)$ for the cross section z = –243 cm at the radius r = 16 cm. The flux $\Gamma(\omega)$ calculated from these functions is shown in Fig. 6. It is clearly seen that the particle flux is produced by oscillations in a narrow frequency range near 10 kHz, whereas, outside this range, either the function $|C(\omega)|$ is small or the phase shift is such that these oscillations do not contribute to the flux. Such a pattern is observed for all radii at the given cross section, whereas the characteristic peak at a frequency of 10 kHz varies in amplitude and changes its sign when the probe is displaced along the radius. Note that, just before the onset of low-frequency oscillations shown in Fig. 3, the calculated flux is an order of magnitude less.

The radial profile of the total particle flux averaged over a series of measurements is presented in Fig. 7. This figure also shows the profiles of the plasma density and the longitudinal-current density, as well as the

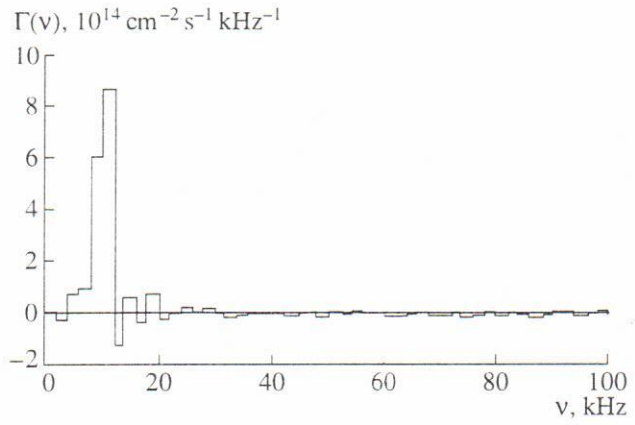

Fig. 6. Frequency dependence of the particle flux at $z = -243$ cm and $r = 16$ cm.

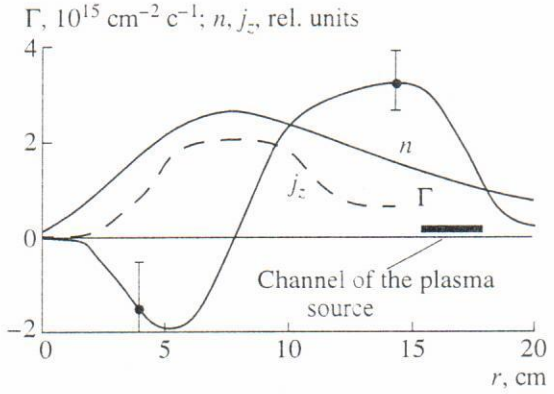

Fig. 7. Radial dependence of the frequency-integrated particle flux at $z = -243$ cm.

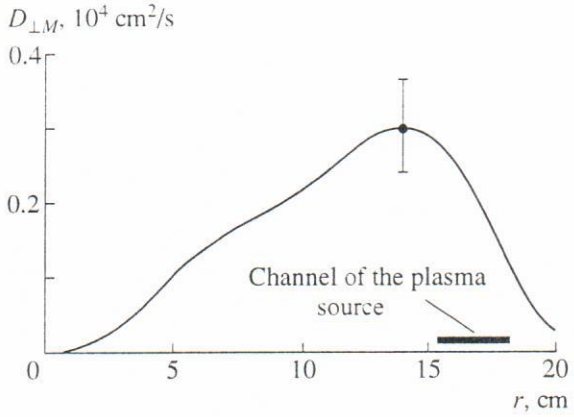

Fig. 8. Radial profile of the diffusion coefficient related to magnetic-field fluctuations at $z = -243$ cm.

projection of the discharge channel of the plasma-source on the magnetic field lines.

Figure 8 presents the diffusion coefficient related to magnetic-field fluctuations determined by the formula $D_{\perp M} \sim -\Gamma/(dn/dr)$ with the use of the experimentally obtained profiles of the plasma density and the particle flux. At the given cross section, the maximum value of the diffusion coefficient related to magnetic-field fluctuations is $D_{\perp M} \approx 0.3 \times 10^4$ cm^2/s, which agrees with the above estimates and is at least an order of magnitude less than the diffusion coefficient related to electrostatic fluctuations.

4. MAGNETIC-FIELD FLUCTUATIONS AND SPATIAL MODULATION OF PLASMA DENSITY

Let us consider now some properties of fluctuations of the azimuthal magnetic field. First, we analyze the frequency spectra of the signals. During the working pulse, the parameters of the plasma-source discharge vary, the plasma is gradually accumulated in the device, and the plasma density and other plasma parameters also vary. Therefore, in fact, the time interval necessary to perform an accurate spectral analysis (i.e., a sufficiently long time interval over which the plasma is in a steady state) is absent. As a consequence, we have to restrict ourselves to considering a relatively narrow time interval $T \leqslant 250$ μs; this leads to poor spectral resolution $\Delta\nu \sim 1/T$. Under the conditions of our experiments, this resolution is 4 kHz. Figure 9 shows the spectra of fluctuations of the azimuthal magnetic field in the transport region, which were obtained by the Fourier transform of the signals measured experimentally in two different cross sections. Both spectra show narrow peaks in the low-frequency region, which are most pronounced at $z = -168$ cm. These peaks, which substantially exceed the background level, are probably associated with the KHI. Although the spectra are plotted on the same scale, it is difficult to compare their amplitudes, because the plasma density decreases by two orders of magnitude over the distance from the source to the input mirror, whereas the electron flow velocity, in contrast, increases. Since the generated magnetic field depends on the combination of these parameters, the absolute calibration of the spectra can hardly be performed. Nevertheless, we can conclude that the spectra contain pronounced low-frequency peaks and the spectral density decreases rather rapidly with frequency.

Spectral analysis gives information about the distribution of the fluctuation energy over frequency. However, it is convenient to introduce one more characteristic of the fluctuating field in which oscillations with various frequencies are present, namely, the root-mean-square value of this field over the time interval T:

$$\langle \tilde{B} \rangle \equiv \left(\frac{1}{T} \int_0^T \tilde{B}^2(t)\,dt \right)^{1/2}.$$

In this case, the time-independent component and the component linearly dependent on time are subtracted

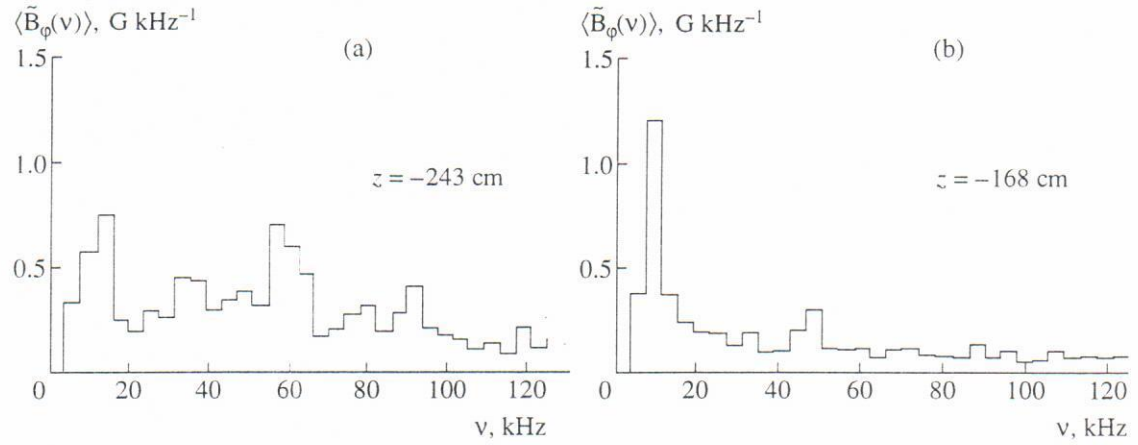

Fig. 9. Spectra of fluctuations of the azimuthal magnetic field in cross sections $z = -243$ cm ($r = 9$ cm) and $z = -168$ cm ($r = 7$ cm) at $t = 1600$ μs.

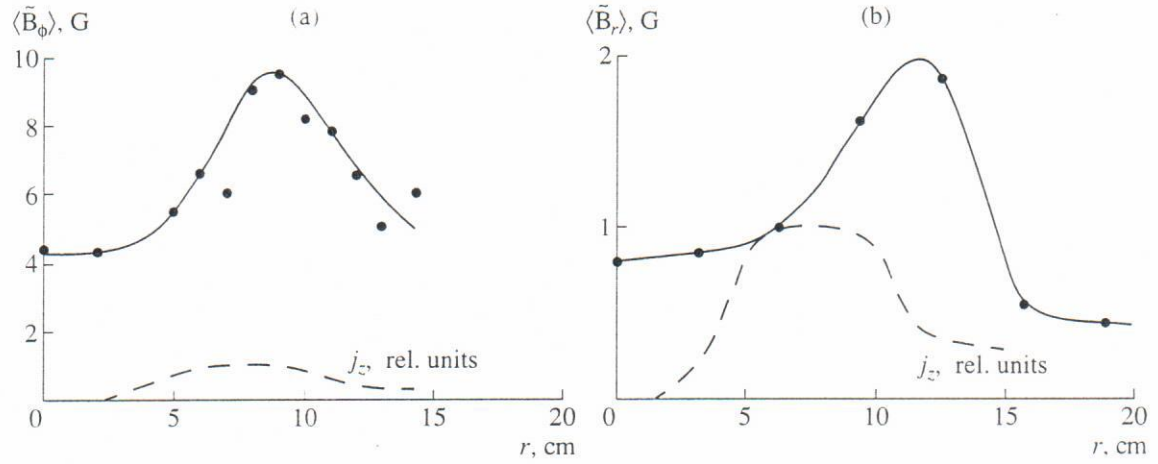

Fig. 10. Radial profiles of the root-mean-square fluctuations of the (a) azimuthal and (b) radial components of the magnetic field. Dashed line shows the current density profile in relative units.

from the initial signal before averaging. Figure 10 presents the radial profiles of the root-mean-square magnetic field fluctuations averaged over the time interval $T = 250$ μs in the vicinity of the instant 1400 μs. In this figure, the current density profiles (in relative units) are also shown for comparison. It is seen in Fig. 10 that the magnetic-field fluctuations in the cross section $z = -243$ cm are rather large even near the axis, where the current density is equal to zero.

There are various mechanisms for the generation of the radial magnetic field measured by a magnetic probe. First, while the plasma is filling the device, the magnetic field varies compared to the vacuum one. This effect can be broken into two ones: the variations in the absolute value of the field and the change in its direction, i.e., in the shape of the field lines. If we know the pressure distribution in the system, then from the condition of the transverse plasma equilibrium under the paraxial approximation $B_z^2(r, z) + 8\pi p_\perp(r, z) = B_v^2(z)$ (where $B_v(z)$ is the vacuum field at the axis of the system) we can calculate both the distribution of the magnetic field and the corresponding shape of the field lines. The correction to the radial magnetic field, which corresponds to the change in the inclination of the field lines, is $\delta B_{r1} \sim B_{vz}\delta\alpha$ (here, α is the inclination angle of the field line and δ stands for the perturbation of a quantity due to the plasma occurrence), whereas the correction related to the change in the absolute value of the field is $\delta B_{r2} \sim \delta B_{vz}\alpha \sim -\alpha 4\pi p_\perp / B_v$. Both of these corrections are proportional to the radius; i.e., they vanish on the axis of the device. In our case, the analysis of equilibrium shows that the change in the inclination of the field lines is more important factor and the calculated correction to the magnetic field corresponds to the experimentally measured radial magnetic field both in value and in sign.

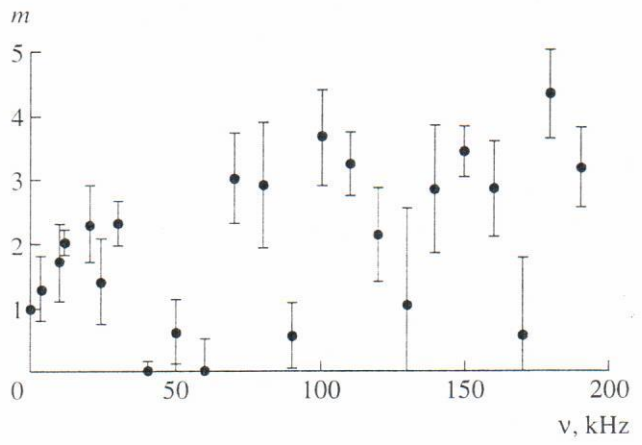

Fig. 11. The azimuthal mode number determined from the radial dependence of the radial magnetic field $B_r \propto r^{-(m+1)}$ at $z = -243$ cm.

Second, the radial magnetic field is produced due to the azimuthal asymmetry of the longitudinal current. This asymmetry can occur, for example, as a result of the azimuthal modulation of the density of electrons carrying the current ($j_1 = n_1 e u_{\|ez}$: the index 1 stands for the perturbation of the corresponding quantity). In the previous section, it was shown that the plasma density and the radial magnetic field have similar spectra with peaks at the same frequencies and correlate with each other. Let us consider the azimuthally nonuniform perturbation of the current density $j_1(r, \varphi) = j_1(r)\cos(m\varphi - \omega t)$, where m is the number of the azimuthal harmonic and the function $j_1(r)$ describes the radial profile of the perturbed current density. From $j_1(r, \varphi)$ we find the dependences $B_{1r}(r, \varphi)$and $B_{1r}(r, \varphi)$. The magnetic field on the axis is determined only by the mode $m = 1$; this allows us to estimate the current density perturbation corresponding to this mode. For the sake of simplicity, we consider a stepwise radial profile of the current density, so the function $j_1(r)$ is constant and nonzero only within the ring $r_1 < r < r_2$. Simple calculations show that, if the interior of the current density profile is hollow, i.e., $r_1 > 0$ (a hollow current cylinder), then, inside this cylinder, the magnetic field created by the current is independent of the radius. For $r > r_1$, the field decreases monotonically, and, outside the space occupied by the current (for $r > r_2$), the field decreases as $B_r \propto r^{-(m+1)}$. A similar picture is observed in the cross section $z = -243$ cm (Fig. 10), in which the inner part of the plasma column is still not filled with the current and the fluctuating magnetic field is almost constant in the region $0 < r < 4$ cm, where the current density is equal to zero. If we know the amplitude of the magnetic field B_r of oscillations with $m = 1$ at $r = 0$, we can find the amplitude of the first mode of the current density j_1. Assuming the radial profile of the current- density fluctuations to be equilibrium, from the experimentally determined current profile we can estimate r_1 and r_2. By taking into account the values of the magnetic- field fluctuations on the axis, the current-density fluctuations in the cross section $z = -243$ cm for the equilibrium current density $j_1 \simeq 2$ A/cm^2 can be estimated as $j_0 \simeq 4$ A/cm^2.

The magnetic field of fluctuations with the azimuthal numbers $m > 1$ is equal to zero on the axis, it reaches its maximum at a certain radius and decreases outside the region occupied by the current. Therefore, as a rule, the experimentally measured profile of the magnetic-field fluctuations, which includes all of the azimuthal modes, reaches its maximum at a certain distance from the axis.

The azimuthal structure of the density fluctuations can be, in principle, determined from the phase shift between signals of two probes located at the same radius in close azimuthal positions. However, we used another method. If the plasma density perturbation depends on the angle as $\exp(im\varphi)$, then, outside the region occupied by the current, the magnetic field decreases as $B_r \propto r^{-(m+1)}$. Therefore, by measuring the radial dependence of the spectral amplitude of the magnetic field at a certain frequency, it is possible to find the mode number corresponding to this frequency. The dependence $m(\omega)$ obtained by this method is presented in Fig. 11. A large scatter in experimental points is seemingly associated with the fact that the values of $m(\omega)$ are not averaged over the ensemble of measurements. It is seen that the mode number is $m = 1$–2 in the frequency range below 50 kHz, in which the most intense fluctuations of the magnetic field are observed in experiment, and it increases to $m = 4$ as the frequency increases to $\nu \simeq 200$ kHz.

5. CONCLUSION

By using movable magnetic probes, we have experimentally studied the fluctuations of the azimuthal and radial magnetic fields and determined their characteristic properties. The radial profile of the particle flux associated with the radial magnetic field fluctuations in the transport region has been measured. The corresponding transverse diffusion coefficient has been estimated.

An analysis of spectra and radial profiles of magnetic-field and density fluctuations shows that the magnetic field fluctuations are associated with modulation of the density and current in the plasma stream. The characteristic azimuthal mode numbers of plasma inhomogeneities are $m = 1$–2, and the current density modulation is about 50%.

ACKNOWLEDGMENTS

We are grateful to G.I. Dimov for continued interest in this work and valuable remarks and to V.S. Belkin for useful discussion. This work was supported in part by

the Russian Foundation for Basic Research, project nos. 95-02-05316 and 96-02-19296.

REFERENCES

1. Dimov, G.I., *Vopr. At. Nauki Tekh., Ser.: Term. Sintez*, 1990, vol. 1, p. 19.
2. Belkin, V.S., Bender, E.D., Gilev, E.A., *et al.*, *Proc. Int. Conf. on Open Plasma Systems for Fusion*, Novosibirsk, 1993, p. 37.
3. Akhmetov, T.D., Belkin, V.S., Bender, E.D., *et al.*, *Fiz. Plazmy*, 1997, vol. 23, p. 988 [*Plasma Phys. Rep.* (Engl. transl.), vol. 23, p. 911].
4. Akhmetov, T.D., Davydenko, V.I., Kabantsev, A.A., *et al.*, *Fiz. Plazmy*, 1999, vol. 25 (in press).
5. Zweben, S.J., Menyuk, C.R., and Taylor, R.J., *Phys. Rev. Lett.*, 1979, vol. 42, p. 1270.
6. Giannone, L., Gross, R.C., and Hutchinson, I.H., *Nucl. Fusion*, 1987, vol. 27, p. 2085.
7. Graessle, D.E., Prager, S.C., and Dexter, R.N., *Phys. Fluids B*, 1991, vol. 3, p. 2626.
8. Liewer, P.C., *Nucl. Fusion*, 1985, vol. 25, p. 543.
9. Rempel, T.D., Almagri, A.F., Assadi, S., *et al.*, *Phys. Fluids B*, 1992, vol. 4, p. 2136.
10. Fiksel, G., Prager, S.C., Pribyl, P., *et al.*, *Phys. Rev. Lett.*, 1995, vol. 75, p. 3866.
11. Kabantsev, A.A. and Taskaev, S.Yu., *Fiz. Plazmy*, 1990, vol. 16, p. 700 [*Sov. J. Plasma Phys.* (Engl. transl.), vol. 16, p. 406].
12. Kabantsev, A.A, *Preprint of Budker Inst. of Nuclear Physics, Siberian Division, Russ. Acad. Sci.*, Novosibirsk, 1995, no. 95-80.

Translated by A. D. Smirnova